Heliyon 10 (2024) e31308

Contents lists available at ScienceDirect

Heliyon

journal homepage: www.cell.com/heliyon

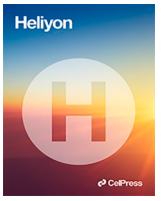

Research article

A novel subsurface slopes hazardous mapping with engineering geologic and geophysical characterizations

Mohamad Anuri Ghazali [a,b], Mohd Rozi Umor [a], John Stephen Kayode [c,*], Abd Ghani Rafek [b], Mohd Hariri Arifin [a]

[a] *Program Geologi, Department of Earth Science and Natural Resources, Faculty of Science and Technology, Universiti Kebangsaan Malaysia, 43600, Bangi, Selangor, Malaysia*
[b] *Geo Mag Engineering. No. 31B, Tingkat 2, Jalan Pelabur B 23/B Seksyen 23, 40300, Shah Alam, Selangor, Malaysia*
[c] *Department of Physics, Nigerian Army University, Biu, No 1, Gombe road, PMB 1500, Biu, Borno State, Nigeria*

ARTICLE INFO

Keywords:
Engineering geology
Geoelectrical mapping
Hazardous slopes mapping
Slope assessment system peninsular Malaysia

ABSTRACT

Engineering geological characterizations, and geophysical mapping of subsurface structures to monitor some susceptible infrastructural facilities to hazardous slopes for effectiveness, safety to lives and properties, in addition to policy management for sustainable development. Novel integrated engineering geology, geoelectrical resistivity (ER), and borehole data analysis, to characterize subsurface for slope instability, determining critical zones prone to hazardous slopes in Peninsular Malaysian (PM), east coast areas was focused on. Engineering Laboratory soil investigations using disturbed and undisturbed samples collected to obtain firsthand information on the subsurface soils, and rocks physical properties, integrated with ER data to obtain subsurface geoelectric profiles. Regions delineated as loose and marked as water saturated residual soils prone to slopes corresponds to ER values < 100 Ω-m. ER values between $100 \geq 500$ Ω-m, were delineated as residual soils zones devoid of water contents. Subsurface geoelectric profiles related to hard materials were delineated as weathered and fractured bedrock zones corresponding to ER values between $500 \geq 2000$ Ω-m. Granitic bedrock units delineated as subsurface lithological zones with ER values > 4000 Ω-m. Slope Mass Ratings (SMR), was carried out to construct suitability, and slope assessment system (SAS) model ratings map for the four classes obtained.

Environmental implications

The dominant high hazard slope ratings recorded at the study sites caused loss of infrastructural valuables and human lives. In recent findings, large number of occurrences of widespread natural disasters worldwide were due to landslide's phenomena caused by hazardous slopes. This study is to prevent an unanticipated threat of the harmful slopes to the environment, ecosystems, infrastructural facilities, as well as human lives. The resultant scale movements of large and small subsurface sediments, either in the sliding downwards or upwards directions are associated with catastrophic damaging effects to the structural facilities at the surface resulting in large scale environmental impact.

* Corresponding author.
E-mail addresses: jskayode@gmail.com, john.kayode@naub.edu.ng (J.S. Kayode).

https://doi.org/10.1016/j.heliyon.2024.e31308
Received 28 May 2023; Received in revised form 14 May 2024; Accepted 14 May 2024
Available online 16 May 2024

1. Introduction

Large mass movements of soils and subsurface rocks occasioned by the influence of gravitational actions from geologic, geomorphologic, and hydrological activities within the subsurface structures. Seismic activities are also part of the natural phenomenon that causes landslides in various parts of the world. Effects of landslides on infrastructural facilities are becoming increasingly alarming, not just in Malaysia, but in the larger world, which is greatly losing valuables and humans to the devastating effects. In recent findings, large number of occurrences of widespread natural disasters worldwide were due to the landslide's phenomena, e.g., Refs. [1–7].

Increase in exploration activities, population explosion, couple with physical structural growth, occasioned by a great number of people competing for undersized portions of available lands for industrial, social and infrastructural development as a result of urbanisation, put a lot of pressure on the subsurface soils and rocks, thereby causing the mass movements of the weak/loose zones, e.g., Refs. [2,3,7]. Subsurface soils, in addition to rocks in regions of intense precipitation are on a regular basis, under powerful pressure related to water permeation leading to the mass movements of saturated soils and subsurface rocks layers. The resultant scale movements of large and small subsurface sediments, either in the sliding or upwards directions are associated with catastrophic damaging effects at the surface. During continuous heavy precipitation, most especially in tropical rain forest zones, the subsurface invariably becomes too saturated as the water reaches the contact plane which triggers unbalance of the mass of soils and subsurface rocks layers. The process of finding equilibrium point causes the mass saturated soil strata to slip at the weak/loose zones causing slope forming materials. It is on this note that engineering geological characterization and mapping of the subsurface structures to identify the soil strata and geomorphological lithological units which paved the way for runoffs are crucial to assessment of slopes/landslides.

Recent improvements to the subsurface mapping using integrated approach, paved the way to the production of high resolution and quality images of structural lithological units in places previously considered inaccessible, such as rugged tropical rain forests terrain. Acquisitions of geological and geophysical data have been made less stressful, more rapid, less expensive, more accurate and consistent for improved investigations. For this reason, an application of the combined geological, geophysical, and in-situ geotechnical engineering tests of soils and subsurface rock layers to estimate slopes/landslides will give a more reliable and higher quality output. This is because geotechnical borehole surveys alone are not sufficient to give the necessary details as they are limited to the diminutive portions of the subsurface soils and rocks layers. The heterogeneous nature of subsurface soil strata requires that the details are captured. Application of the subsurface integrated mapping approach has been reported to be the best method of sampling the details of subsurface geologic structural lithological units for financially viable and time-saving approach, e.g., Refs. [2–4,6–9].

When the details information about the subsurface structural networks are required for a large area coverage, geophysical surveys have been extensively applied for costs effectiveness and fast acquisition of favourable parameters that influenced occurrences of

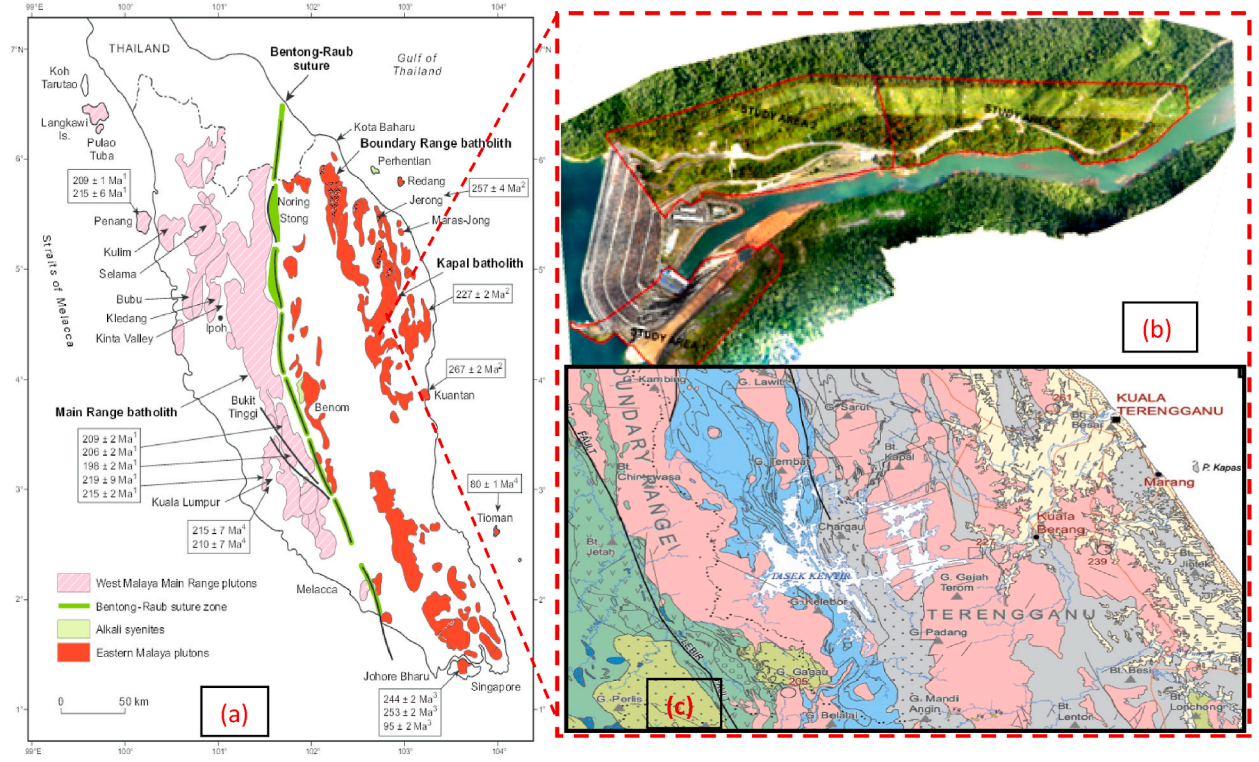

Fig. 1. (a) Geological map of PM showing, (b) Location of the study areas, and (c) the local geology map of Terengganu. Modified from Ref. [15].

weak, or loose soils stratum materials causing slope/landslides formations. Recently [7], applied a 4-D electrical resistivity tomography (ERT), to assessed influence of plants and subsurface vapour on the railway cutting conditions, and slope stability in the UK. They reported a shrink-swell behaviour of clay subsurface soils of the railway cuttings that resulted in fissures and shear strength reductions that caused slope stability. On the other hand [6], used unmanned aerial vehicle (UAV), to map out and detect slopes and possible hazards associated with the present study area. On the other hand [9], applied a novel method to classified structural anisotropy in jointed rock masses, utilising theoretical rock conditions to designate formulation adjusted to combined spacings. In Ref. [3]' the authors applied digital elevation model and ERT analysis to reconstruct landslide movements in the Polish Outer Carpathians. They showed in their reports that the ERT geophysical measurements delineated varied resistivity of the rock formations proving that landslides were created because of the atmospheric and geologic conditions of the subsurface of the Polish Outer Carpathians. Ref. [4] used integration of electrical resistivity and multi-channel analysis of surface waves (MASW), to characterize subsurface soil materials for landslide studies. However [10], studied groundwater contaminations and its unintended consequences with the use of surfactant-enhanced mobilization of determined organic pollutants as prospect for soils and sediments remediation.

Engineering geological characterization, and geophysical mapping of the study area's subsurface structures was carried out at the *Janaelektrik Sultan Mahmud Station, Kenyir, Terengganu*, Peninsular Malaysia, to study discontinuities and uniaxial compressive strength of the surveyed areas. The study area is principally made up of infrastructural facilities like operational, and office buildings, roads, and spillway. The site was alienated into three sections that comprises: (a) rock dominated slopes within the heavy urbanise areas, (b) mixtures of rock and soil slopes, and lastly, (c) the soil dominated slopes within the pylon and thick vegetation areas. The study site consists of cut-slopes, embankments, and naturally occurring slopes, e.g., Fig. 1. ER surveys of the mapped areas were carried out to define the actual subsurface resistivity by the inversion of the computed field apparent resistivity values recorded with the aid of a computer inversion programme, e.g., Refs. [11–14]. A two dimensional (RES2DINV), geoelectric subsurface resistivity imaging/tomography with large numbers of electrodes was used to survey the study areas' complex lithological units.

Application of geophysical methods as a pre-construction assessment of the subsurface geological structures, most importantly the ER methods to thoroughly access the earth materials prior to engineering constructions works. The use of ER is principally due to their cost effectiveness, robustness, non-intrusive and timesaving. Siting of any engineering structures must be preceded with geoelectrical studies of the subsurface lithological formations because of the resistivity variations of the earth materials. Measurement of ER and the 2DINV models generated must be correlated with the borehole logs produced for the subsurface lithological sections [16,17].

In the study, ER method was applied to assess the knowledge of the geological structures underlain the areas covered, to simplify the characterization, and classification of the rock mass properties. Application of the physical quantities obtained from the ER helped to quantify zones with hazardous slopes which served as greater significant for the rock mass classifications scheme. Although, we could not completely rule out ambiguities from the subsurface geophysical parameters recorded during the field data acquisition, post field data processing, and data validation, due to some humans and instruments errors, coupled with the subsurface structural conditions of the lithological units. These problems were surmountable by integrating geophysical data with the in-situ borehole well logs to accurately evaluate the underground lithological units. However, as a well-known geophysical method, ER was used to image the hazardous slopes that are very crucial to engineering development thereby proffer suggestions to the policy makers, engineering construction firms, graphic-originators, and geophysical/geological explorers at the study sites [16–18].

Slope Mass Ratings (SMR) were carried out, which help with the construction of suitability, and slope assessment system (SAS) model ratings map of the study area by applying the methods reported in [9,19–21]'. The globally accepted system of communique by engineering construction firms, graphic-originators, and geophysical/geological explorers, to simplify data for the rock mass properties, description, and sorting, utilises the much-publicised slope mass classification systems, with the Rock Quality Designation (RQD), and SMR. The system offers qualitative data and strategies for driving geomechanically classifications in engineering construction works, using none complicated but efficient, methodological approach to representing SMR. On a general note, e.g. Refs. [20,22,23], reported that classification of rock mass is one of the important parameters to be considered for the determination of the slope geometry. Consequent upon this, RQD was hence considered as a valued quantity. and standard parameter in the measurement of core logs from the ground surface down to the bottom of the borehole during the site investigation prior to the SMR determinations. The combination of kinematic and SMR methods helped to easily mapped out the fragmented regions, determination of the geo-engineering characteristics for the assessment of each of the slopes within the subsurface lithological units.

1.1. Novelty of the research

Application of SMR, integrated with geophysical exploration is novel because it constituted a basis for innovative modern rocks, and slopes classification systems. In addition, the methodological approach is believed to be a foundation for initiation of new innovative rocks, and slopes mass classification systems. The novelty of the adopted approach in this research lies on assessments of rocks, and slopes mass environments for the sole purpose of engineering construction works. Besides, straightforward communiqué involving diverse clients, decision-makers, and policy formulations. The novelty allowed preparation of details and complete stability charts with the aid of extensive geo-field surveys. The development of SMR provides thorough, and accurate analysis of slopes in critical weak zones that are associated with geological units, in-situ stress conditions, geo-engineering indexes, and weathering impacts that are prone to hazardous slopes.

2. Materials and methods

2.1. The study area

To understand the causes of slopes and failures in the study area, it is important to review the geology of the subsurface lithology and the slope steepness as the causative factors with precipitation as the generating factor. Geological mapping of rocks and soils exposure with all pertinent geological and geodynamic features such as weathering profiles, structural and relic discontinuities data collection from the available outcrops along the slope cuts and any water seepage on the slopes was carried out at the study area. The study area was divided into three locations which comprise areas of interest as shown in Fig. 1b.

1) Study site 1 was covered with rock slopes and heavily developed area. The operation room, office and transformer at the *Janaelektrik Sultan Mahmud* Station are located in this area.
2) The study site 2, is sparsely covered by rock slopes, pylon, and a thick forest area.
3) The third study site is mostly covered by thick vegetation and pylon.

The power transmission lines pass through both study site 2 and 3 on the hilly area.

The study areas are characterized by undulating mountainous topographic terrains gridded by the PM, Rectified Skew Orthomorphic (RSO) formations, via the Kertau 1948 Datum system with varied altitudes from 100 to 320 m, above mean sea level (MSL). The land-use comprises thick forests mostly covered by palms and rubber plantations.

The PM is principally made up of two terrains that trend north to south and originated from the Gondwana terrain due to the deferential in their magma composition, mineralization stratigraphic, and structural sequences. They are (a) westerly *Sibumasu* terrain, and (b) the easterly Sukhothai-Indochina terrain, e.g., Refs. [14,24]. The *Bentong-Raub* Suture Central Belt Zone (BRSZ), mostly characterized by the Devonian to Middle Triassic Paleo-Tethys oceans that divided the two terrains which is through subduction of the Paleo-Tethys Ocean beneath the *Sukhothai Indochina* when it collides with Sibumasu terrain all through the early Permian and Triassic era. These terrains were reported to be part of one supercontinent under Gondwana through paleo-biogeographic and tectonic stratigraphic classifications, but got spilled at various era of Phanerozoic ages, e.g. Refs. [15,25,26]'. Because of the depositional scale characteristics, regional geochemical and geological settings, PM was reported to be principally composed of Cambrian to Ordovician classic sediments that showed typical Permian Gondwana originated from the North-western Australian Plate, e.g., Refs. [15,26].

The local geology of *Kenyir* study area which covered the whole catchment regions of the Terengganu River, comprises series of the sedimentary rocks that are mostly sandstones and shales, with metamorphic rocks that are primarily quartzites and phyllites, intruded by granitic masses. By and large, the catchment area is underlain by felsic igneous rocks that mostly consists of granites and granodiorites, marine clastics, e.g., (shales and sandstones), minor carbonates with some embedded metamorphics rocks, e.g., (phyllites and quartzites), basic to intermediate volcanic rocks. However, the eastern section of the Kenyir Lake, is underlain by granitic rocks of the Kapal batholith. The batholith is a composite rock body ranging from diorites to monzogranites in composition and mostly dominated by granodiorites. Fig. 1c, shows the regional geology map of the Terengganu areas.

The strike of fold axes for the sedimentary rocks are approximately in the NW to NNW directions. However, the catchment area witnessed a syncline strike that are mostly along the NNW directions. But the granite witnessed numerous dolerite dykes' intrusions with strike directions stretching from NE to eastern zones. Though, barely minor faulting was encountered in this area, but the *Kenyir* Dam site and its eight saddle dams were all sited in the granitic terrains. At the main dam site, however, the underlying bedrock comprises of localised coarse-grained biotite granites with different dolerite dykes. The dykes have varying widths that generally ranged from 5 cm to as much as 2 m, that strikes along the NE to E directions through vertical or sub-vertical dips. The dolerite dykes stretched from 30 to 100 m, and then disappeared, before showing pinching or en-enchelon features. They are mostly fresh at the sides or walls of the valley, but are weathered where previously submerged under the river, such as at the bottom of the valley at the dam foundation area. Jointing of the granite is rather intensive. At the main dam site, there are three major sets of joints, two with vertical or sub-vertical dips striking NNE and SSE directions, and one set with horizontal or sub-horizontal dips, striking parallel to the valley. The joint spacings varied from 0.6 m to 1.6 m, weathered, and exposed at the surface with intermittent clay materials filling up the joints. At a deeper depth detected from the borehole wells, however, the joints are fresher and closer together.

2.2. Methods of data acquisition

The soil investigation was carried out to acquire in-situ information on the physical properties of the subsurface soils and rocks underneath the study area, for the engineering geological characterization and geophysical mapping of the study area for subsurface conditions arising from geo-structural distress, and damages to earthworks such as infrastructural facilities like operational, and office buildings, roads, and spillway caused by slopes/landslides. Data for the subsurface conditions and subsurface profile information were obtained at the 3 sites using borehole, and geoelectrical resistivity methods of geophysical survey to map the study area.

The engineering geological mapping, and the site assessment were undertaken in walk-over surveys. The relevant geological features such as subsurface lithology types, geo-structural discontinuities, degree of weathering, and the existence of projected geotechnical problems were noted, and recorded during the field mapping. Collection of the geological data for the study areas were divided into building some of the scanline, combined with the engineering geological information, and plotted them on the map. To evaluate the potential of the rock slope failures, kinematic analysis was performed on all the collected data for discontinuity tests. Whereas for the purpose of assessing the degree of weathering, and rock strengths at the field, Schmidt hammer test was used. The

Slope Mass Ratings (SMR), of the study area was carried out using the methods reported by, [9,19–21].

The discontinuities data and geological features for rock slopes were collected using the scanline method. Scanline was built at every 30 m length along the slope and was named chainage. The structural features were recorded on the sketch, based map, and survey drawings. Close-up photographs of the relevant geological and geotechnical features, such as hanging block, fractured rocks and joints were captured together.

2.3. Laboratory test

Laboratory tests were carried out on selected samples collected from 17 boreholes from the sites, Fig. 2.

Size and Depth of Boreholes: The size of boreholes, e.g., 100 mm diameter, was such that all the in-situ testing and sampling were satisfactorily carried out as required.

Sampling in the Boreholes: Soil samples for the distress zones were collected via split spoon-sampler, equipped with flap, and other attachments necessary for fewer cohesion soils. Enough soil samples were collected from each borehole to carry out various classification tests.

Rotary drilling, where the drill bit or casing shoe is spin at the base inside the well. The drilling fluid which is pumped down to the bit through the hollow drill rods, lubricates the bit and flushes the drill debris up to the ground surface of the well. Water is used as drilling fluid. Rotary core drilling is providing a rock core sample. Rotary open hole drilling is suitable when speedy spread of a borehole is required for field testing, and instruments installation.

Double-tube core barrels were used with pertinency, though with some restrictions. This was used with an inner tube mounted on bearings that does not rotate against the core to moderately decompose the rocks. The core is removed by hanging the barrel in a near vertical position and tapping on the sides of the barrel. In highly fractured rocks, this can result in a jumble of rock fragments in the core box. The rock core samples were also found and placed in the core box for logging.

2.3.1. Filed testing

2.3.1.1. Standard penetration test (SPT). The SPT, Fig. 3, was implemented in accordance with the International British Standard Test No. 19 B S 1377:1975. Determination of the penetration resistance using split core barrel sampler and self-tripping hammer of

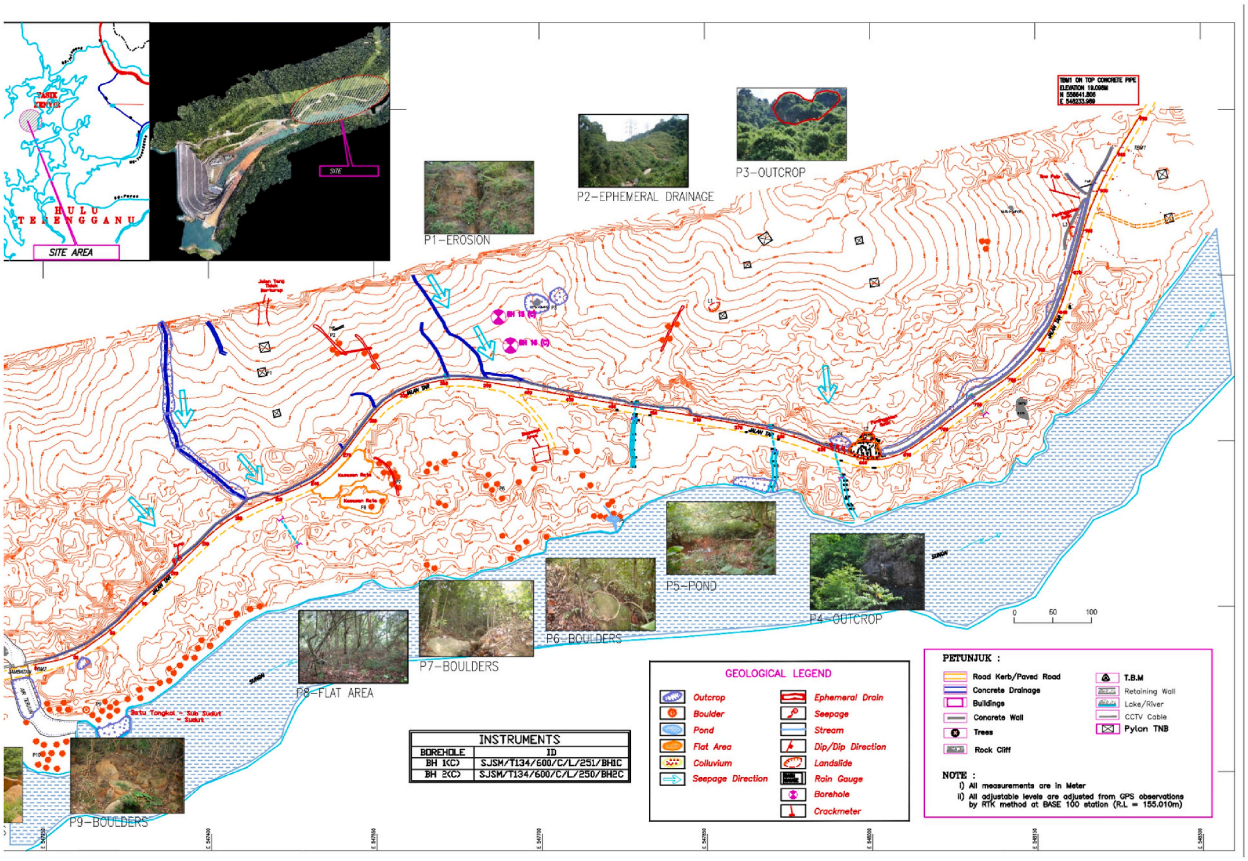

Fig. 2. Topographical map of the site showing the borehole location points.

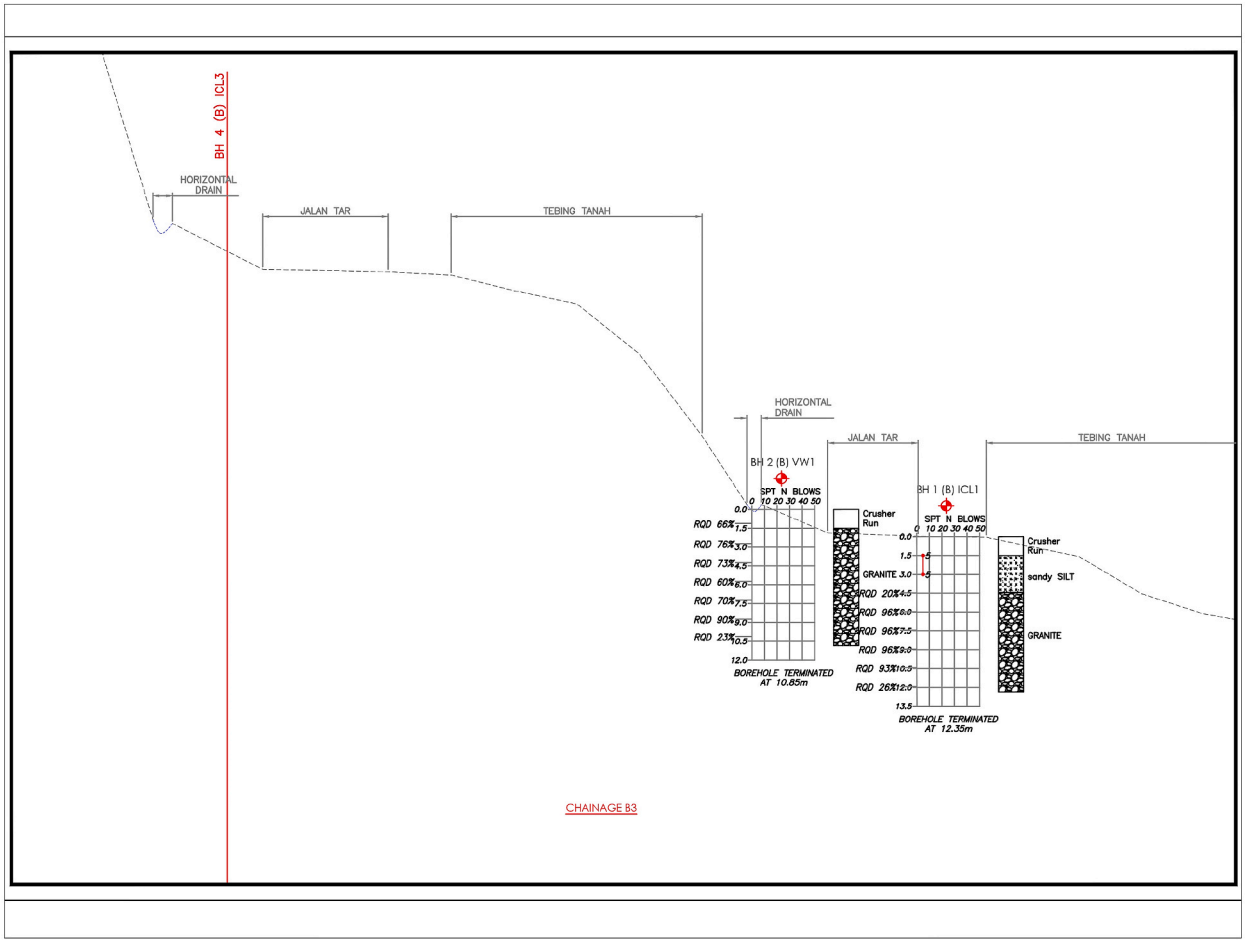

Fig. 3. A typical SPT plot, showing the cross-section of slope and the borehole.

approved design.

By and large, SPT was performed in all the types of soil present, except for the very soft silts, and soft clays, at 1.5 m intervals or change of strata or as instructed by the Site Officer.

The value of N as defined by the BS method was reported together with the number of blow counts for each 75 mm penetration of the sampling tube. The blow count for the first 150 mm penetration (e.g., the setting drive), which does not contribute to the value of N was also included.

2.3.1.2. Permeability test. Determination of the in-situ permeability tests in boreholes involved the applications of hydraulic pressure in the borehole different from that on the ground surface. The pressure in borehole increases due to the introduction of water into it, calling falling head or inflow test. When the pressure is held constant during test, i.e., (constant-head test), and equalize to its original value, (e.g., variable-head test). This approximate value reflected the infiltration capacity of the subsurface materials.

2.3.1.3. Packer test. The packer test gives a measure of the acceptance by in-situ rock of water under pressure. It comprises the measurement of the volume of water that can escape from an uncased section of the borehole in a given time under a given pressure. The test is used to assess the amount of grout that the rock will accept.

2.3.2. Resistivity survey

18 lines of geoelectrical resistivity surveys were conducted to study the subsurface slope profile that could be a threat at the Sultan Mahmud Power Station, Terengganu, PM. The first electrode position was marked as 'A' and the last electrode marked as 'B', whilst the electrode at the centre of survey line was marked as 'C'. The alignment of the survey lines is as shown in Fig. 4.

In general, all the geoelectrical resistivity lines were divided into three groups of study areas. Fig. 4 showed the division of the resistivity lines at the study sites. Each ER line has a maximum of 200 m survey spread length with 5.0 m inter electrodes spacing for a total of 41 electrodes per each survey line. A Global Positioning System (GPS) was used to record the coordinates and elevations of the electrodes positions during the field data collections.

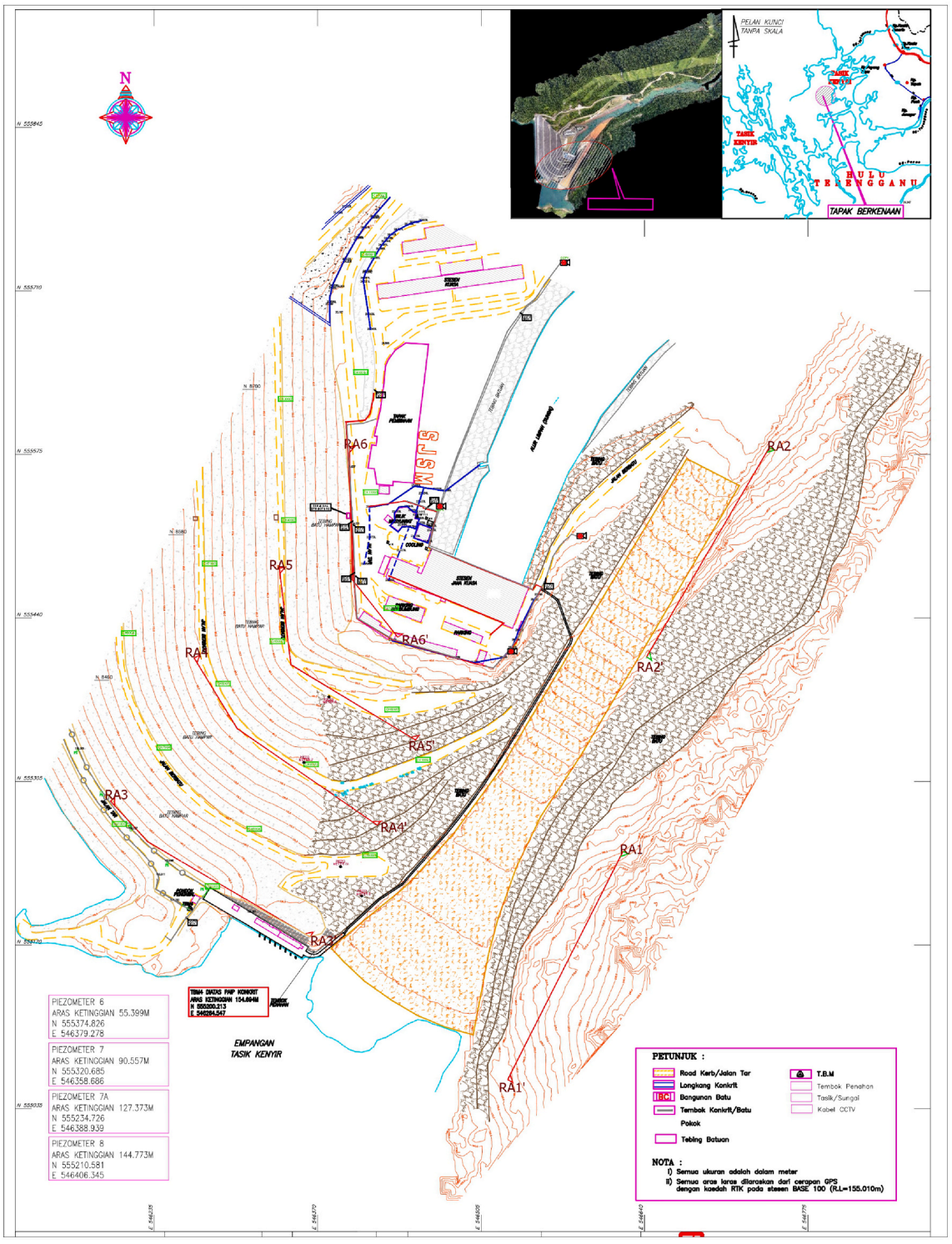

Fig. 4. Layout of ER survey lines distribution at the study area.

3. Results and discussion

3.1. Electrical resistivity (ER), survey results

Based on the ER values recorded, the subsurface materials underlain the study area can be classified into four zones as summarized below.

1. Recorded resistivity values < 100 Ω-m related to the loose, and water-saturated residual soils. This was marked as **water saturated zone.** The zone was indicated by dark blue to light-blue colours coding on the subsurface RES2DINV profiles plots.
2. Resistivity values obtained between 100 and 500 Ω-m was related to the residual soil devoid of water contents or dry zone and marked as **Residual soils.** The unit consists of subsurface materials considered as soft to moderately hard geologic unit. Green colour code was used to indicate the zone on the subsurface RES2DINV profiles. Water saturated channels were delineated within this zone.
3. Resistivity values recorded for between 500 and 2000 Ω-m was interpreted as the hard subsurface lithological materials that are highly weathered or fractured bedrock. The unit was marked as **weathered/fractured granites zone** on the RES2DINV profiles. The recorded resistivity values were coded by the yellowish to orange colours as shown.
4. Resistivity values recorded >4000 Ω-m was interpreted as the hard lithological materials or weathered bedrock with a smaller amount of fractured or non-fractured. This zone was marked as the **fresh granites/bedrock unit** on the RES2DINV profiles. The recorded range of resistivity values showed by the red and purple colours coding indicated on the profile plots.

The study of slopes/landslides assessment from subsurface geologic materials that need close attention are the zones with recorded resistivity values that are <500 Ω-m. These subsurface lithological materials are considered as the soft zones that can retain water during intense precipitation and can easily collapse following the slope gradient. Under certain conditions, the weathered/highly fractured granite rocks besides, has the potentials to equally failed because of some subsurface strong motions such as earthquakes and tremors.

From the subsurface ER profile TK RES13 along the survey line presented in Fig. 5 above, with southeast to northwest orientations, it could be concluded that the main components of the profile are residual soils. The fresh granite rock delineated and marked as d, along the survey line as observed before the centre electrode at point C, through to the top right end of the profile, e.g., between 80 and 200 m. The lithological layer was interpreted as the rock fill dam with thickness about 5 m. At the bottom of the subsurface profile, just a little above the centre point, the layer was interpreted as the granite bedrock unit. The observed residual soils are dominant starting from the initial electrode position at point 0 m through to 100 m along the survey line. The gap that separated the residual soil from another big mass of residual soil was filled with highly weathered/fractured granitic rock unit. The other huge mass of residual soil was delineated close to the centre at point C through to about 180 m along the survey line. A water saturated zone was observed at the beginning of the ER up to about 50 m along the profile. Whereas weathered or fractured granitic unit was observed to be evenly distributed from the middle of ER profile TK RES13 to the end part of the profile.

Fig. 6 showed the recorded subsurface ER values along the survey profile line TK RES14 on southeast to northwest directions. From the RES2DINV, the whole section of the profile was underlain by weathered and fresh granitic bedrock units. From the first electrode position at point A to the centre point along the survey line, a granitic layer with a thickness of approximately 60 m was delineated as the bedrock lithological unit. The second main features delineated was interpreted as the rock fill dam. This lithological layer could be

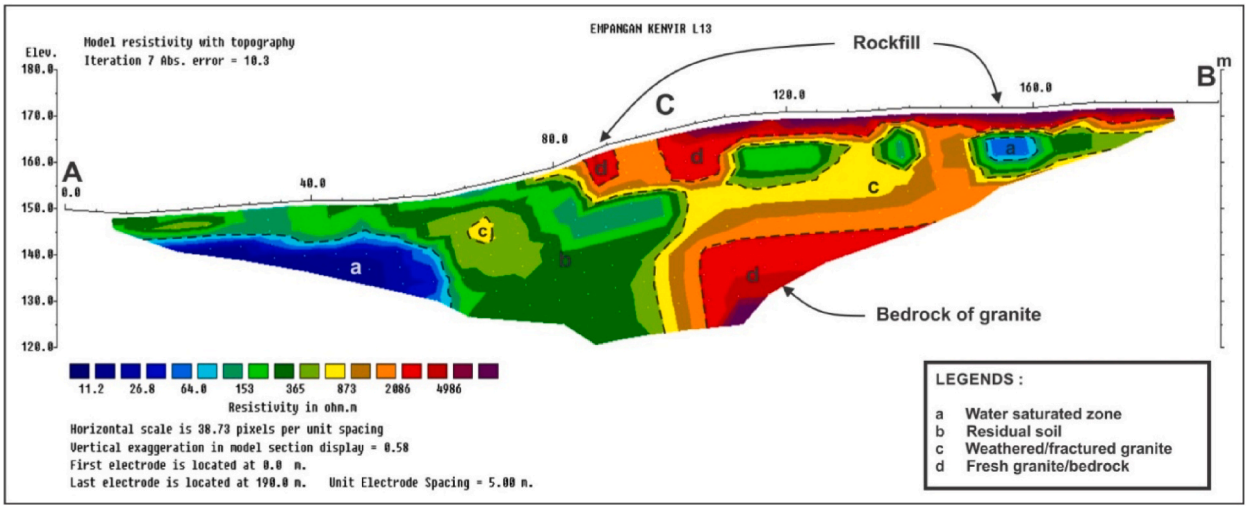

Fig. 5. ER survey across the subsurface profile line TK RES13 of the study area.

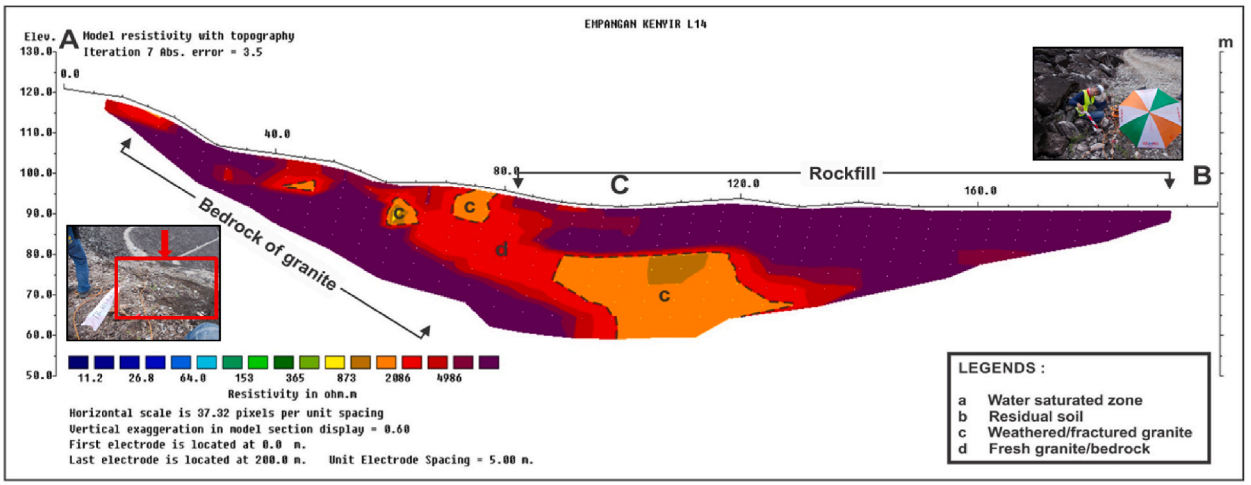

Fig. 6. ER survey across the subsurface profile line TK RES14 of the study area.

observed at a distance of about 85 m from the initial electrode at point A through to the last electrode at point B with thickness of about 20 m. At the centre of the survey line TK RES14, a weathered or fractured granitic lithological unit was delineated with approximate thickness of about 68 m.

The ER subsurface profile along survey line TK RES15, as presented in Fig. 7, and orientated from southeast to northwest of the study area, was interpreted as fresh granitic/bedrock lithological unit for the entire geoelectrical section with recorded resistivity values $>$ 5000 Ω-m. A highly weathered/fractured granitic and residual soil units with the bedrock as the most dominant features along the profile with a thickness of about 50 m with geoelectrical resistivity values that are 2000 $\leq$ 4000 Ω-m. At the northwest section of the profile, a few weathered or fractured granites were observed which also subsist in the subsurface granitic bedrock unit. The delineated inconsequential feature observed in the profile was a residual soil with a thickness of about 5 m. The bedrock lithological unit was observed to be exceptionally homogenous, and hence, was considered as a stable subsurface unit in the area.

On the basis of the geoelectrical resistivity values recorded along the subsurface profile TK RES16, from southeast to northwest directions of the study area as shown in Fig. 8, the profile presented high resistivity values recorded at the top layers that varied from 2000 Ω-m $\leq$ 4000 Ω-m. The top layers were interpreted as a hardpan filled materials that was used during the road construction works. The recorded resistivity values of $>$2000 Ω-m and the thickness of about 5 m, (e.g., paved road), to 45 m, (e.g., rock fill dam), with other layers overlapping it. Within these lithological layers, some granitic boulders were randomly distributed as observed at the ground surface that is supposed to be a rock-fill dam. The second delineated lithological layers were interpreted as the residual soils with resistivity values of $<$500 Ω-m. The layers were observed at a surface distance of about 10 m, and up to 110 m deep as observed along the north-eastern directions of the subsurface profile. Weathered, and fractured granitic units were observed mostly at the south-

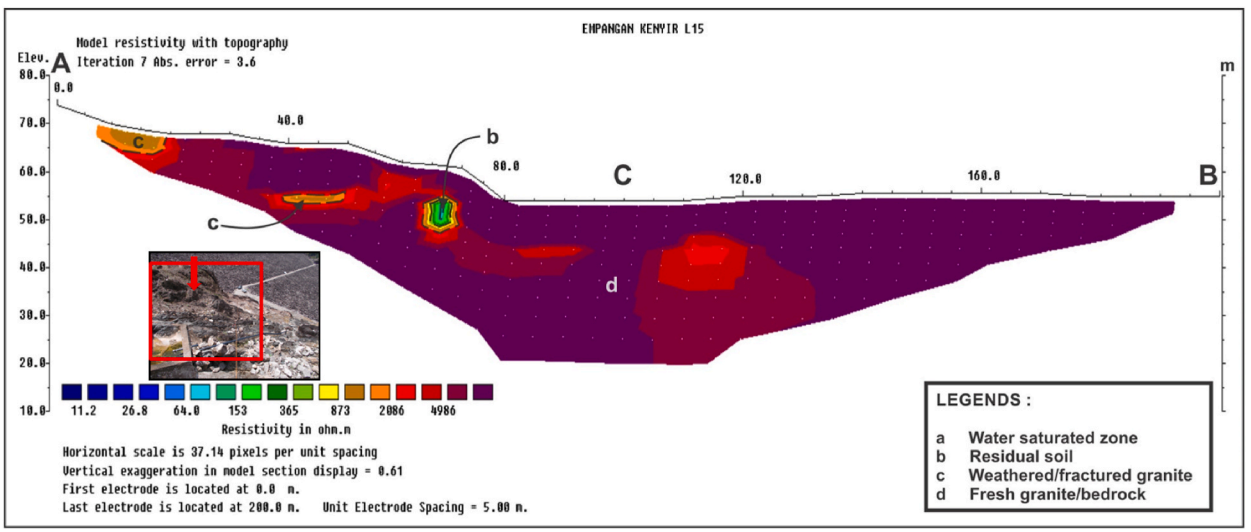

Fig. 7. ER survey across the subsurface profile line TK RES15 of the study area.

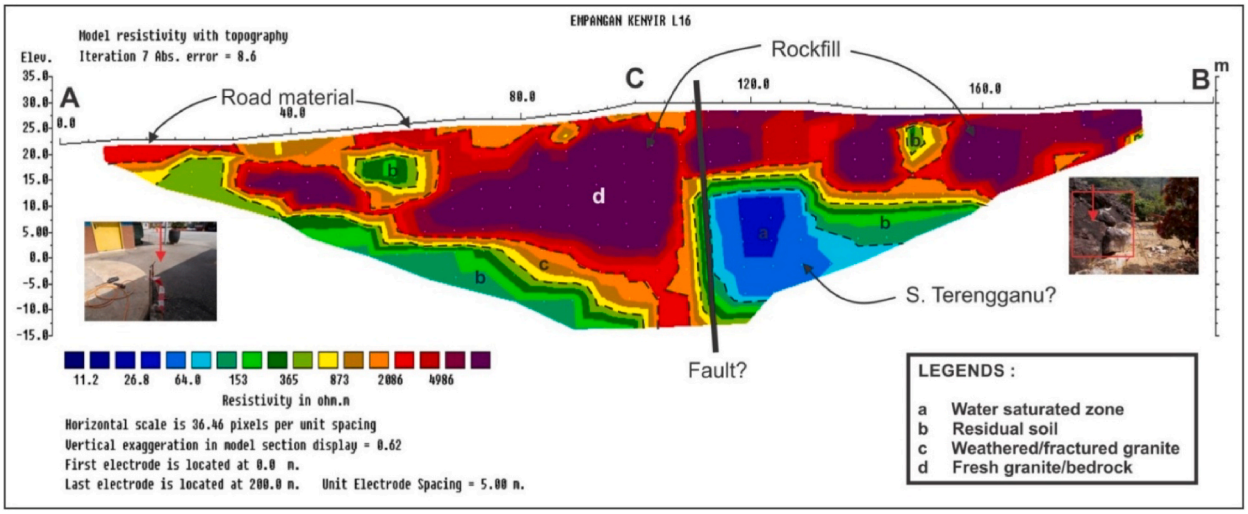

Fig. 8. ER survey across the subsurface profile line TK RES16 of the study area.

western directions of the subsurface geoelectric profile. The water saturated zone was found within this layer at the south-eastern section of the subsurface geoelectric profile. The large water saturated zone was delineated along the survey line at about 115–130 m from the centre point C at depth of about 15 m. The subsurface unit was sited underneath the hardpan filled materials which could likely be the former River channels, (e.g., Sungai Terengganu). A probable fault in the vicinity of the central position at point C with a slight displacement of the fresh granitic layers as observed at the top of the geoelectric profile.

The geoelectric resistivity survey line TK RES18 along the northeast to southwest directions of the study area is presented in Fig. 9. Based on the geoelectric profile, nearly half of the lithological layers were made up of fresh granitic bedrock as delineated at the south-western part of the survey line. The recorded thickness was about 30 m, with high resistivity values that varied from 4000 Ω-m $\leq$ 6000 Ω-m starting from the initial electrode position at A, 0 m, to the centre point at C. The residual soils at the north-eastern part occurred as isolated body within the highly weathered/fractured granitic lithological layers. The water saturated zone is shallow at the central point C, at an estimated depth of about 5.0 m. Water saturated zones became deeper towards the survey line end at point B, and the depth was estimated to be $>$ 10 m. The water saturated zones were caused by the presence of seepage conduit on the outcrop next to the spillway as shown on Fig. 9.

Fig. 10 shows the geoelectric resistivity survey line TK RES3 along the west to the east directions and parallel to the main road. The most important subsurface component delineated was the fresh granitic bedrock lithological unit as the bottom layer with thickness of

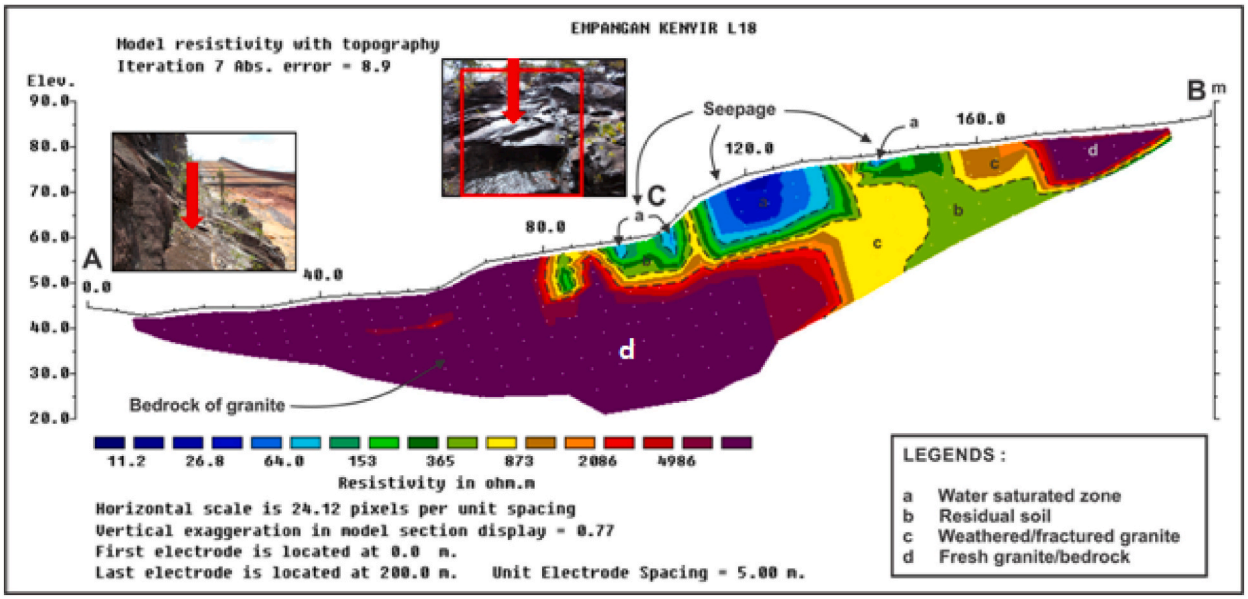

Fig. 9. ER survey across the subsurface profile line TK RES18 of the study area.

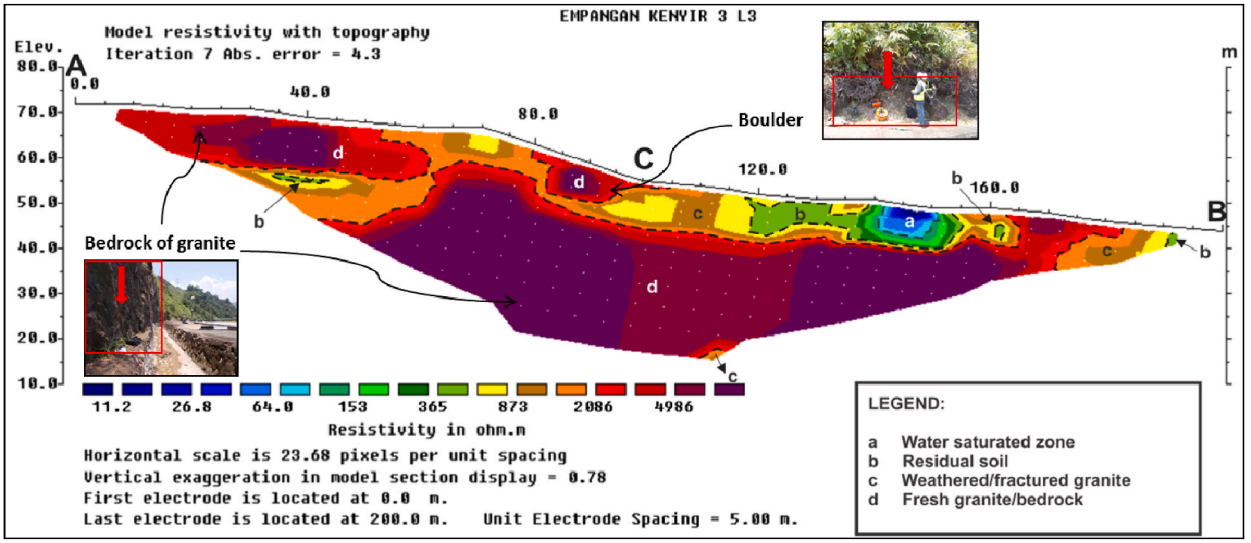

Fig. 10. ER survey across the subsurface profile line TK RES3 of the study area.

about 50 m, and higher resistivity values that varied from about 5000 Ω-m ≤ 6000 Ω-m. There were two fresh granitic rock bodies that were delineated as boulders at the top of the profile towards the western segment along the survey line. Weathered/fractured granitic lithological layers with thickness of about 10 m, and high resistivity values of about 2000 Ω-m, were delineated at the top section of the bedrock unit. The layers were sited at distances of about 20 m–164 m from the initial point A together with a residual soil zone. Water saturated channels were recorded at about 43 m, 65 m, and from 95 m to 165 m from the starting point A along the survey line. At around 110 m from the initial point A, there appears to be a fractured under the bedrock layer as shown. It shows there could be the possibility of further weathered/fractured granitic layers at deeper probing towards the eastern part of the profile if the survey length is > 200 m.

3.2. *Engineering geological mapping*

The engineering geological mapping, e.g., (Fig. 11), was undertaken to identify the subsurface geological features at the Sultan Mahmud Power Station, Terengganu, PM study sites. The slope discontinuity data were collected to identify elements of instability on the slope, interpret the likely mode of failures and assess the overall stability of the rock slopes. Kinematic rock slope stability analysis was done to study the engineering geological properties of the subsurface geological features underneath the study area, and hence, produce the engineering geological maps that shows potential slope instabilities at the study sites.

Granites with medium-grained textures formed the main subsurface lithological units, with minerals that are mostly >1.0 mm length. The mineral composition consists of quartz, (i.e., 50 %), alkali feldspar, (i.e., 25 %), plagioclase, (i.e., 20 %), biotite, (i.e., <5 %), and some ore minerals, e.g., (<5 %). Om the basis of QAP classifications, the main rocks were identified as granitic rocks. These rocks were considered as felsic rocks. The petrography analysis showed that quartz is the major mineral present in them. From the physical observation, the colour was observed to be light grey, and anhedral textural features, e.g., no shape, but the sizes range between 0.1 mm and 3.0 mm length. There were two different sizes of quartz minerals that were observed, the first occurred as matrix around 0.1 mm, and the second as phenocryst at averagely about 1.0 mm. Closed observations showed that the samples were sheared as a result of faults or stress. We can, therefore, name the rocks as sheared granites.

The results from the kinematic rock slope stability analysis helped to pinpoints areas with potentially weak stability without accompanying forces that could lead to failure, and hence, prediction of the geological properties of the subsurface geo-structural features underneath the study area was made possible. To aid the outcome of this study with a view to characterize the stability of the rock slopes around the study area, we combined kinematic analysis with the SMR to be able to evaluate the types of failure together with the diverse stability classes, and discontinuity parameters. With the combination of these methods, fragmented regions were easily mapped out to be able to determine the geo-engineering characteristics for the assessment of each of the slopes within the subsurface lithological units.

Xenolith were found several metres apart at the study areas. The texture of the xeno-lithological unit is very fine-grained, and mostly consists of minerals that are <0.5 mm in lengths. The mineral composition consists of plagioclase, (i.e., 50 %), pyroxene, (i.e., 10 %), hornblende, (i.e., 10 %), chlorite, (i.e., 30 %), and ore minerals, (i.e., <5 %). From the QAP classifications, the rocks were identified as gabronorites, and pyroxene-hornblendes. These rocks were considered basic rocks. The petrography observations showed that the plagioclase produces grey colours with tabular shapes, and sizes that range between 0.1 mm and 0.2 mm lengths. The plagioclase minerals observed in the xenolith samples were fine, and do not give good quality shapes. However, pyroxene was observed to be the yellowish and orange colours, usually formed in octahedral shapes with various sizes at about 0.1 mm diameter.

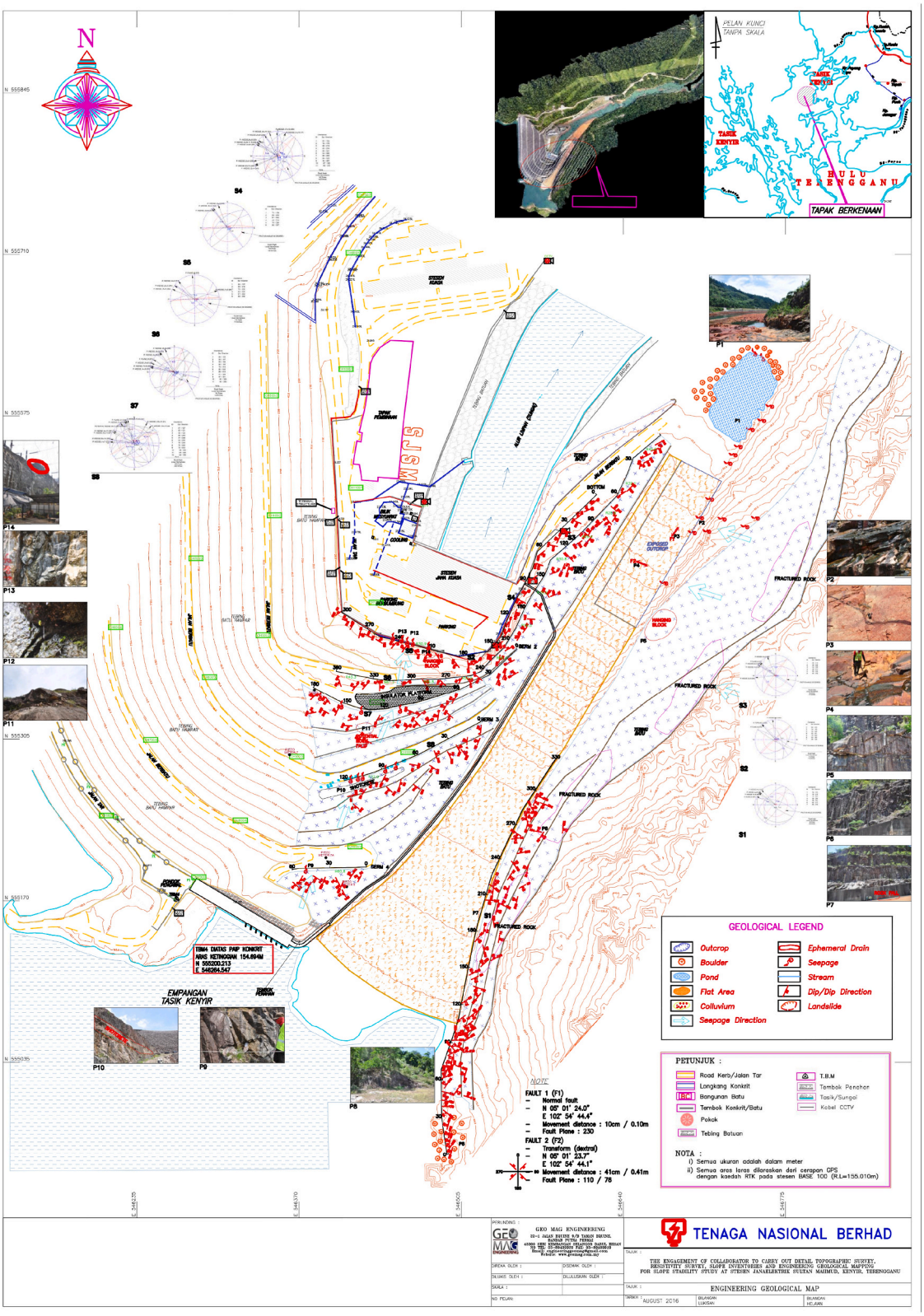

Fig. 11. Engineering geological map of the subsurface rocks underlain the study area.

The observed slopes comprise rock slope occasioned by the blasting and excavation of earth materials to build the platform for the construction of the earth dam, the official residences, office complex, and spillways. Almost the entire slope with a vertical and steep angle but the discontinuity of rock slope features is clear. In some areas, there are water seepages flowing through rock fractures, especially near the car parking area.

3.2.1. Strength of intact rock

To characterize the stability of the rock slopes around the Sultan Mahmud Power Station using the Slope Mass Ratings (SMR), the study area was divided into two environmental settings, (a) the area around the spillway, and (b)the developed dam area. Both areas were studied in detail. The study area was divided into 30 m scan line to ease the *Discontinuity Survey* on each of the slopes. The slopes nearer to the spillway are mostly between 300° and 350° orientations, and for the developed areas, the orientations are in the range of 10°–300°. The main subsurface lithology underneath the study area is Granitic rock bodies. The weathering grades at both study sites was observed to be in the range of slightly to moderately weathered, to moderately weathered; from roughness, to slightly rough and to smooth. Some main faults were also observed at the areas nearer to the spillway, whereas joints were mostly observed to be prominent at the developed dam area. In terms of aperture, both areas have values from 1 mm to 5 mm, and majority of the study area have no infilling between the rock walls of discontinuities. The presence of seepages was mostly observed on slopes close to the spillway, and the parking lots at the developed dam site, while the other areas were observed to be completely dried. All these parameters were significantly taken into account so as to be able to determine the engineering behaviour for the assessment of each of the slopes. The compressive strength recorded in the study area is summarized as presented in Table 1.

In practice most tests on rock outcrops must be done in a horizontal, or near horizontal directions. The average values for the Uniaxial Compressional Strength (UCS), lies between 30 N/mm^2 to 68 N/mm^2 e.g., Ref. [22]. The slopes areas with recorded UCS values of between 50 and 100 N/mm^2 were categorised as strong zones that are sited around the spillway. On the other hand, at the developed dam areas the values of UCS recorded varied from 30 N/mm^2 to 50 N/mm^2. It could be seen that the weathering grade contributes mostly to the parameters that is responsible for the UCS values recorded. The difference in weathering grade of the slopes may perhaps yield such UCS values at the study area. From the UCS values obtained, the strength of intact rock ratings for each slope was computed and presented in Table 2, using the proposed methods by Refs. [19–22,24,27]. The ratings were used for further SMR calculations.

The Rock Quality Designation (RQD), i.e., Table 3, is one of the parameters in computing the SMR. RQD values, ratings were

Table 1
Summary of the compressive strength recorded in the study area.

Location	Chainage	Compressive Strength (N/Mm^2)	Rating
Bottom	0–30	30.19	4
	30–60	40.76	4
	60–90	49.29	4
	90–120	38.43	4
	120–150	65.14	7
	150–180	64.57	7
	180–210	59.14	7
	210–240	59.71	7
	240–270	57.71	7
	270–300	52.29	7
Top	0–30	33.10	4
	30–60	47.76	7
	60–90	50.33	7
	90–120	29.29	4
	120–150	48.29	4
	150–180	56.29	7
	180–210	55.14	7
	210–240	41.00	4
	240–270	43.71	4
	270–300	49.43	4
	300–330	66.00	7
	330–360	66.86	7
Berm 2	0–30	67.14	7
	30–60	65.14	7
	60–90	61.43	7
	90–120	69.43	7
	120–150	66.00	7
	150–180	68.86	7
Berm 3	0–30	65.14	7
	30–60	58.00	7
	60–90	63.00	7
	90–120	63.00	7
Berm 4	0–30	67.43	7
	30–60	62.86	7
	30–60	63.29	7

Table 2
Strength of intact rock ratings.

Qualitative Description	Uniaxial Compressive Strength (MPa)	Point Load Test (MPa)	Ratings
Strongest	>250	8	15
Stronger	100–200	4–8	12
Strong	50–100	2–4	7
Moderate	25–50	1–2	4
Weak	5–25	–	2
Weaker	1–5	–	1
Weakest	<1	–	0

Table 3
Summary of rock quality designation.

Location	Chainage	Rock Quality Designation (M)	Ratings
Bottom	0–30	15.6	3
	30–60	11.1	3
	60–90	24.9	3
	90–120	19.5	3
	120–150	19.4	3
	150–180	16.7	3
	180–210	30.6	8
	210–240	30.9	8
	240–270	25	8
	270–300	28.1	8
Top	0–30	45.6	8
	30–60	35.1	8
	60–90	28.8	3
	90–120	26.4	3
	120–150	30.8	8
	150–180	15.2	3
	180–210	34.3	3
	210–240	66.4	13
	240–270	52.6	13
	270–300	46.8	8
	300–330	61.2	13
	330–360	43.3	8
Berm 2	0–30	36.7	8
	30–60	36.7	8
	60–90	30.8	8
	90–120	32.9	8
	120–150	35.2	8
	150–180	30.9	8
Berm 3	0–30	31.9	8
	30–60	35.5	8
	60–90	62.0	13
	90–120	62.0	13
Berm 4	0–30	60.8	13
	30–60	60.8	13

obtained as proposed by Refs. [9,19,20]. RQD recorded at the study sites as presented in Table 4, which range from 15 m to 60 m, that is, from very poor to moderately good. The recorded ratings for developed dam areas shows RQD from very poor to poor with ratings from 3 m to 8 m. Whereas, the slopes near the spillway yield RQD values that range from 35 m to 60 m, e.g., poor to moderately good.

In general, the overall ratings recorded for the study area varies between very poor to moderately good. Factors that contribute to such results could possibly be the spacing between the subsurface structural discontinuities.

Table 4
Rock quality designation (RQD) ratings.

Rock Quality	RQD	Ratings
Perfect	90–100	20
Good	75–90	17
Moderate	50–75	13
Poor	25–50	8
Very Poor	<25	3

3.2.2. Spacing of discontinuities ratings

The spacing of adjacent discontinuities is mostly controlled by the size of individual blocks of intact rocks. Several closely spaced sets are likely to give conditions of low mass cohesion. Whereas those that are widely spaced are much more likely to yield interlocking conditions. These effects are a function of the persistence of the individual discontinuities present in the particular subsurface structural unit under testing. As in the case of orientations, the importance of spacing increases when other conditions for deformation are present, as a typical example, low shear strength, and an adequate number of discontinuities or joints sets for slip to occur.

The spacing of individual discontinuities and associated sets, Table 5, has a strong influence on the mass permeability and seepage characteristics. In general, spacing of discontinuities is the distance between them, and is measured along a line perpendicular to the discontinuity planes. Throughout the fieldwork it was observed that the Aperture recorded for the study area varied mostly between 1 and 5 mm.

3.2.3. Condition of discontinuities (persistence)

Persistence implies the areal extent or size of a discontinuity within a plane. It can be crudely quantified by observing the discontinuity trace lengths on exposures at the ground surface. It is one of the most important rock mass parameters, but one of the most difficult to quantify in any engineering materials except in crude terms. The discontinuities of one particular set will often be more continuous than those of the other sets. Therefore, the minor sets tend to terminate against the primary features, or they could be terminated in solid rocks.

Frequently, rock exposures are smaller in comparison to the area or length of persistence discontinuities, and the real persistence can only be guessed. Less frequently, it may be possible to record the dip length and the strike length of exposed discontinuities, and their persistence along a given plane, though the rock mass could be estimated using the probability theory. However, the difficulties and uncertainties involved in the field measurements will be considerable for most rock exposures encountered. From the fieldwork, it was inferred that the persistence discontinuities of the study area, Table 6, is between 1 m and 10 m.

3.2.4. Slope gradient attributes

The slope gradient attributes (SGA) map was generated by using the ArcGIS software 10.3.1 version from the ESRI Malaysia as the base map. The slope gradient was given in degrees, and classified into six (6) groups, and the data was summarized as presented in Table 7. The slope angle for each terrain units was measured along the directions of the greatest declivity. The direction normal to the contour lines, enables the identification of the most limiting slope angle. In general, the mapped study area consisted of approximately 18.96 acres of land, i.e., (26.78 %), of recorded slopes up to 5°. About 2.84 acres, i.e., (4.01 %), of the study area has recorded slope of between 5°–15°. Moderate slope gradient of between >15° and 25° which covered about 2.23 acres, e.g., (3.16 %). For slope gradient >25°–35°, it covered approximately 20.81 acres, e.g., (29.40 %), whereas slope gradient >35°–60° covered about 17.78 acres, e.g., (25.12 %). For recorded slope gradient >60°, it covered about 8.16 acres, i.e., (11.53 %).

3.2.5. Construction of suitability map

The suitability map of the study area was constructed from the data recorded for four classes produced out of the geological terrain classifications, e.g., Table 8. Class I covered by approximately 22.15 acres of lands or 31.30 % and has low geotechnical limitations. Class II area covers 2.23 acres or 3.16 % of the study area. The development in the class II area requires moderate geotechnical and geological studies due to the geotechnical limitations which is moderate and requires normal intensity of site investigation. There is about 20.81 acres or 29.40 % grouped in Class III. Class III area requires high geotechnical and geological studies and hence, more attention should be put on this area to enable development. Erosion and minor instabilities are expected in the slopes, but these can be readily mitigated. Generally, construction in these areas is not expected to encounter any major foundation problems. Lastly, Class IV in study area consists of 25.59 acres which is 36.15 % of the total study area of 70.78 acres.

3.2.6. Slope assessment system (SAS) Model-B

The SAS Model-B is frequently used by Malaysian *Jabatan Kerja Raya* (JKR), and widely accepted with the assessment of the slope's instability or the probability of failure or landslides occurrences. SAS Model-B is usually divided into 4 types of hazard ratings based on the instability score as shown in Table 9.

The slope hazard ratings were further simplified into the slope or polygon map by filing each of the delineated slopes with colour coding, (i.e., alert type), with respect to each of their respective hazard ratings as shown in Table 10.

The geological hazard slope assessment site investigation was conducted by qualified geologists and geophysicists on each of these reported slopes by thorough inspection based on the data obtained from engineering geological characterization and geophysical mapping of the study area. The instability scores were computed, and the results are presented in the geohazard map shown in Fig. 12.

4. Conclusions

On the basis of the principal objective of the research work through the application of novel geological engineering integrated with electrical resistivity (ER) geophysical subsurface mapping, and borehole Laboratory data analysis, was conducted to characterize the subsurface slope instability by determining the critical zones prone to slopes in PM east coast areas. Based on the results produced as shown in Fig. 12, there were obvious visible proofs of the occurrence of all types of slope hazards ratings at the study sites based on the SAS model-B methods adopted for the studies. It is on this basis that the results produced, extremely low hazards, low hazards, high hazards, and exceptionally high hazards as marked by the blue, green, orange, and red colours coding respectively on the SAS

Table 5
Rating for spacing of discontinuities.

Spacing of Discontinuities	Ratings
>2 m	20
0.6–2 m	15
200–600 mm	10
60–200 mm	8
<60 mm	5

Table 6
Persistence Ratings for the study area.

Persistence	<1 m	1.3 m	3–10 m	10–20 m	>20 m
Ratings	6	4	2	1	0

Table 7
Summary of the SGA recorded at the study area.

Slope Gradient	Group	Area	
		Acre	%
0°–5°	1	18.96	26.78
>5°–15°	2	2.84	4.01
>15°–25°	3	2.23	3.16
>25°–35°	4	20.81	29.40
>35°–60°	5	17.78	25.12
>60°	6	8.16	11.53
Total		70.78	100.00

Table 8
Summary of the construction of suitability classes recorded at the study area.

Suitability Class	Suitability for Development	Geotechnical Limitation	Area	
			acre	%
Class I	High	Low	22.15	31.30
Class II	Moderate	Moderate	2.23	3.15
Class III	Low	High	20.81	29.40
Class IV	Probably Unsuitable	Extreme	25.59	36.15
Total			70.78	100.00

Table 9
Hazard rating designed for the SAS Model-B.

Instability Score	Hazard Rating
2.137–2.653	Very High
1.620–2.137	High
1.005–1.620	Low
0.389–1.005	Very Low

Table 10
Slope hazard ratings and colour coding.

Instability Category	Colour (Alert Type)
Very Low	Blue
Low	Orange
High	Orange
Very High	Red

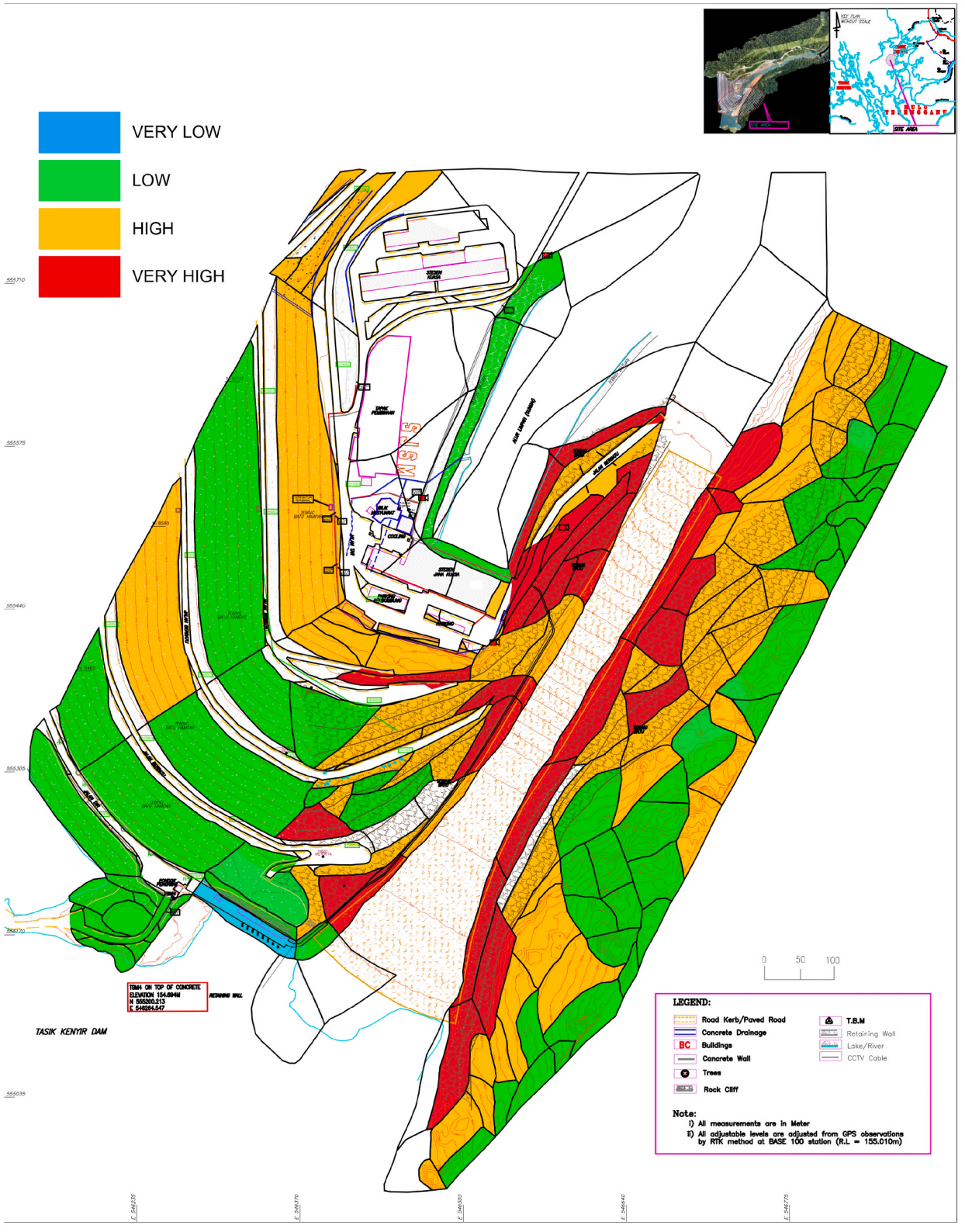

Fig. 12. Geohazard map from the Slope Assessment System (SAS), model.

geohazards map produced.

The most dominant high hazard slope ratings were located near the spillways. The potential cause for the contribution of high hazard slope ratings varied depending on the slope angle, vegetation cover condition, presence of failure on the slope or embankment, and presence of water seepage. Steep angle such as $> 63^{\circ}$ usually give a high instability score, consequently, causing high hazard ratings. Some high hazard slope ratings also caused by exposed slope cover conditions usually <80 %, (e.g., areas with no vegetation cover), causing erosions to easily occur, and hence, giving rise to the slope failure.

Low hazard slopes mostly dominate around the Janaelektrik Sultan Mahmud Station, Kenyir, Terengganu, roadsides, and on flatland areas at the study sites. Low hazard slopes also appear in the areas with remedial works such as rock-fills, horizontal drains, and proper drainage systems such as cascade drains, and berm drains system, thus lowering the instability score. Besides these systems, some of the other natural slopes also show a wide distribution of low hazards slope ratings as coded by the greenish colour on the map. The contributing factors responsible for lowering the instability score for the natural slopes, such as less steep slope angle, and very good vegetation cover conditions are completely absent at the red zones as indicated. Therefore, it is not uncommon for natural slopes to have low hazard ratings in view of the fact that the potential of slope failures could occur when the slope angle is steeper, typically more than 45° without any slope protection.

Consequently, gentle slopes with steep angle less than 35° are more stable compared to steep slope, lowering the probability of occurrences of failures. A good vegetation cover conditions will minimize the activities of erosion as it prevents occurrences of slope failures. Erosion is commonly known as the main agent contributing to the occurrences of slope failure globally in tropical rain forests areas that are constantly experiencing intense precipitation almost all year rounds. Geological model for the study area has been developed based on the work done through topographic survey, geoelectrical resistivity survey, slope inventories, and engineering geological mapping. The geological model shows that the triggering factor in the study area is naturally induced by intense rainfalls. The overall results helped to infer the hazard slopes zones which reflected the field observations of the subsurface geo-structural lithologic instability conditions. Proper drainage systems on the slopes, remediation works for damaged rock slopes and soil slopes require urgent attention. Mitigating works for the potential geo-hazards' zones need to be done instantaneously.

Declaration section

We wish to draw the attention of the Editor to the following facts which may be considered as potential conflicts of interest, and to some significant financial contributions to this work.

Ethics approval

Review and/or approval by an ethics committee was not needed for this study because this manuscript does not involve either experimental animals or human patients. We further confirm that any aspect of the work covered has been conducted with the ethical approval of all relevant bodies and that such approvals are acknowledged within the manuscript.

Funding

There is no funding for this project in the forms of grants from any agencies in the government, local or federal, public, commercial, or not-for-profit organizations.

Consent to publish

We confirm that we have given due consideration to the protection of intellectual property associated with this work and that there are no impediments to publication, including the timing of publication, with respect to intellectual property. In so doing we confirm that we have followed the regulations of our respective institutions concerning intellectual property as it affects this publication.

Data availability

All the data generated or analysed during this study is hereby included as supplementary material to be publish in Data-In-Brief Journal.

CRediT authorship contribution statement

Mohamad Anuri Ghazali: Supervision, Project administration, Methodology, Investigation, Funding acquisition, Formal analysis, Data curation, Conceptualization. **Mohd Rozi Umor:** Software, Resources, Project administration, Investigation, Funding acquisition, Formal analysis, Data curation. **John Stephen Kayode:** Writing – review & editing, Writing – original draft, Visualization, Methodology, Investigation, Conceptualization. **Abd Ghani Rafek:** Visualization, Software, Resources, Formal analysis, Data curation. **Mohd Hariri Arifin:** Validation, Software, Resources, Project administration, Methodology, Formal analysis, Data curation, Conceptualization.

Declaration of competing interest

We wish to draw the attention of the Editor to the following facts which may be considered as potential conflicts of interest, and to some significant financial contributions to this work. We wish to confirm that there are no known conflicts of interest associated with this publication, and there had been no significant financial support for this work that could have influenced its outcome.

We confirm that the manuscript have been read and approved by all named authors and that there are no other persons who satisfied the criteria for authorship but are not listed. We further confirm that the order of authors listed in the manuscript was approved by all the authors.

We confirm that we have given due consideration to the protection of intellectual property associated with this work and that there are no impediments to publication, including the timing of publication, with respect to intellectual property. In so doing we confirm that we have followed the regulations of our institutions concerning intellectual property.

We further confirm that any aspect of the work covered in this manuscript that involved either experimental animals or human patients has been conducted with the ethical approval of all relevant bodies and that such approvals are acknowledged within the manuscript.

We understand that the Corresponding Author is the sole contact for the Editorial process (including Editorial Manager and direct communications with the office). He is responsible for communicating with the other authors about progress, submissions of revisions and final approval of proofs. We confirm that we have provided a current, correct email address which is accessible by the Corresponding Author, and have been configured to accept email from him.

Acknowledgement

The authors wish to sincerely appreciate GEO MAG ENGINEERING, and KUMPULAN IKRAM, for the approval to share the data, and all that helped towards the field data acquisition. We equally appreciate the efforts of all editors and reviewers for their editorial contributions that improved the quality of the paper.

References

[1] P.O. Falae, D.P. Kanungo, P.K.S. Chauhan, R.K. Dash, Electrical resistivity tomography (ERT) based subsurface characterisation of Pakhi Landslide, Garhwal Himalayas, India, Environ. Earth Sci. 78 (14) (2019) 1–18, https://doi.org/10.1007/s12665-019-8430-x.

[2] P.O. Falae, R.K. Dash, D.P. Kanungo, P.K.S. Chauhan, Interpretation on water seepage and degree of weathering in a landslide based on pre-and post-monsoon electrical resistivity tomography, Near Surf. Geophys. 19 (3) (2021) 315–333, https://doi.org/10.1002/nsg.12142.

[3] J. Cebulski, B. Pasierb, D. Wieczorek, A. Zieliński, Reconstruction of landslide movements using digital elevation model and electrical resistivity tomography analysis in the Polish Outer Carpathians, Catena 195 (2020) 104758, https://doi.org/10.1016/j.catena.2020.104758.

[4] Y. Hussain, O. Hamza, M. Cárdenas-Soto, W.R. Borges, J. Dou, J.F.R. Rebolledo, R.L. Prado, Characterization of Sobradinho landslide in fluvial valley using MASW and ERT methods, REM-International Engineering Journal 73 (2020) 487–497, https://doi.org/10.1590/0370-44672019730109.

[5] R.K. Dash, D.P. Kanungo, J.P. Malet, Runout modelling and hazard assessment of Tangni debris flow in Garhwal Himalayas, India, Environ. Earth Sci. 80 (9) (2021) 1–19, https://doi.org/10.1007/s12665-021-09637-z.

[6] M.F. Zolkepli, M.F. Ishak, M.S. Wahap, The application of unmanned aerial vehicles (UAV) for slope mapping with the determination of potential slope hazards, in: Design in Maritime Engineering, Springer, Cham, 2022, pp. 45–67, https://doi.org/10.1007/978-3-030-89988-2_5.

[7] J. Holmes, J. Chambers, P. Wilkinson, B. Dashwood, D. Gunn, M. Cimpoiaşu, M. Kirkham, S. Uhlemann, P. Meldrum, O. Kuras, D. Huntley, 4D electrical resistivity tomography for assessing the influence of vegetation and subsurface moisture on railway cutting condition, Eng. Geol. 106790 (2022), https://doi.org/10.1016/j.enggeo.2022.106790.

[8] S. Rebello, A.N. Anoopkumar, E.M. Aneesh, R. Sindhu, P. Binod, S.H. Kim, A. Pandey, Hazardous minerals mining: challenges and solutions, J. Hazard Mater. 402 (15 January 2021) (2021) 123474, https://doi.org/10.1016/j.jhazmat.2020.123474.

[9] H. Sonmez, M. Ercanoglu, G. Dagdelenler, A novel approach to structural anisotropy classification for jointed rock masses using theoretical rock quality designation formulation adjusted to joint spacing, J. Rock Mech. Geotech. Eng. 14 (2) (2022) 329–345, https://doi.org/10.1016/j.jrmge.2021.08.009.

[10] S. Bolan, L.P. Padhye, C.N. Mulligan, E.R. Alonso, R. Saint-Fort, T. Jasemizad, C. Wang, T. Zhang, J. Rinklebe, H. Wang, K.H. Siddique, Surfactant-enhanced mobilization of persistent organic pollutants: potential for soil and sediment remediation and unintended consequences, J. Hazard Mater. (2022) 130189, https://doi.org/10.1016/j.jhazmat.2022.130189.

[11] M.H. Loke, Tutorial: 2-D and 3-D Electrical Imaging Surveys, 2016. http://www.geotomosoft.com.

[12] M.H. Arifin, J.S. Kayode, M.K.I. Ismail, A.M. Abdullah, A. Embrandiri, N.S. Mohd Nazer, A. Azmi, Environmental hazard assessment of industrial waste materials, (IWM), with the applications of RES2-D method and 3-D Oasis Montaj modeling: a case study at Kepong, Kuala Lumpur, Peninsula Malaysia, J. Hazard Mater. 406 (15 March 2021) (2021) 124282, https://doi.org/10.1016/j.jhazmat.2020.124282.

[13] J.S. Kayode, M.H. Arifin, A. Hussin, N. Roslan, Engineering site characterization using multi-electrode electrical resistivity tomography, Sains Malays. 48 (5) (2019) 945–963, https://doi.org/10.17576/jsm-2019-4805-03.

[14] J.S. Kayode, M.H. Arifin, M.B.I. Basori, M.N.M. Nawawi, Gold prospecting mapping in the peninsular Malaysia gold belts, Pure Appl. Geophys. 179 (2022) 3295–3328, https://doi.org/10.1007/s00024-022-03121-w.

[15] M.P. Searle, M.J. Whitehouse, L.J. Robb, A.A. Ghani, C.S. Hutchison, M. Sone, S.P. Ng, M.H. Roselee, S.L. Chung, G.J.H. Oliver, Tectonic evolution of the Sibumasu–Indochina terrane collision zone in Thailand and Malaysia: constraints from new U–Pb zircon chronology of SE Asian tin granitoids, J. Geol. Soc. 169 (4) (2012) 489–500, https://doi.org/10.1144/0016-76492011-107.

[16] J.S. Kayode, M.H. Arifin, M.I. Mansor, N.N.A. Malek, R.C. Musa, S. Shahri, N.H. Izehar, M.R. Umor, Hydrogeophysical modeling of the groundwater aquifer units under climate variability in parts of Peninsular Malaysia: a case study of the climate-water nexus approach to sustainability, Heliyon 9 (3) (2023) e13710, https://doi.org/10.1016/j.heliyon.2023.e13710.

[17] H.A.H. Zaid, M.H. Arifin, N.S.M. Nazer, S.H. Hazim, M.R. Umor, M.A.M. Sidek, A.M. Abdullah, J.S. Kayode, Geophysical investigation for engineering construction assessment in Karst area, Phys. Chem. Earth, Parts A/B/C 129 (2023) 103329, https://doi.org/10.1016/j.pce.2022.103329.

[18] M.H. Arifin, J.S. Kayode, K.I. Abd Rahim, M.A. Asyraf Sulaiman, N.S. Mohd Nazer, Subsidence mapping for sustainable development, and the geologic, structural foundation, and stability Nexus, European Association of Geoscientists & Engineers V2023 (2023) 1–5, https://doi.org/10.3997/2214-4609.202378056. March 2023.

[19] M.R. Romana, A geomechanical classification for slopes: slope mass rating, in: Rock Testing and Site Characterization, Pergamon, 1993, pp. 575–600, https://doi.org/10.1016/B978-0-08-042066-0.50029-X.

[20] R. Tomas, A. Cuenca, M. Cano, J. García-Barba, A graphical approach for slope mass rating (SMR), Eng. Geol. 124 (2012) 67–76, https://doi.org/10.1016/j.enggeo.2011.10.004.
[21] M. Romana, R. Tomás, J.B. Serón, Slope Mass Rating (SMR) geomechanics classification: thirty years review, in: 13th ISRM International Congress of Rock Mechanics, OnePetro, 2015, May. Paper Number: ISRM-13CONGRESS-2015-131.
[22] K.T. Chau, R.H.C. Wong, Uniaxial compressive strength and point load strength of rocks, Int. J. Rock Mech. Min. Sci. Geomech. Abstracts 33 (2) (1996, February) 183–188, https://doi.org/10.1016/0148-9062(95)00056-9. Pergamon.
[23] R. Hack, An evaluation of slope stability classification, November, in: ISRM EUROCK 2002, Publ. Sociedade Portuguesa de Geotecnia, Lisboa, Portugal, 2002, pp. 3–32, 2002.
[24] J. Kundu, K. Sarkar, A.K. Verma, T.N. Singh, Novel methods for quantitative analysis of kinematic stability and slope mass rating in jointed rock slopes with the aid of a new computer application, Bull. Eng. Geol. Environ. 81 (2022) 1–19, https://doi.org/10.1007/s10064-021-02524-8.
[25] C.K. Morley, Late cretaceous–early palaeogene tectonic development of SE asia, Earth Sci. Rev. 115 (1–2) (2012) 37–75, https://doi.org/10.1016/j.earscirev.2012.08.002.
[26] I. Metcalfe, Tectonic evolution of the Malay peninsula, J. Asian Earth Sci. 76 (2013) 195–213, https://doi.org/10.1016/j.jseaes.2012.12.011.
[27] M.F. Zolkepli, M.F. Ishak, M.Y.M. Yunus, M.S.I. Zaini, M.S. Wahap, A.M. Yasin, M.H. Sidik, M.A. Hezmi, Application of unmanned aerial vehicle (UAV) for slope mapping at Pahang Matriculation College, Malaysia, Phys. Chem. Earth, Parts A/B/C 123 (2021) 103003, https://doi.org/10.1016/j.pce.2021.103003.